Automation and Machine Learning (2024) DOI: 10.23977/autml.2024.050210
Clausius Scientific Press, Canada ISSN 2516-5003 Vol. 5 Num. 2

Trajectory Tracking Control of Unmanned Surface Vessel Based on Neural Network Observer

Ang Zheng[1,a,*], Junhan Yang[2,b], Xiaoming Xia[2,c]

[1]Makarov College of Marine Engineering, Jiangsu Ocean University, Lianyungang, Jiangsu, China
[2]College of Marine Engineering, Jiangsu Ocean University, Lianyungang, Jiangsu, China
[a]2022221712@jou.edu.cn, [b]1302272826@qq.com, [c]xiaxiaoming@jou.edu.cn
[*]Corresponding author

Keywords: Neural network state observer, Unmanned ship motion control, uncertain term, Lyapunov function

Abstract: In this paper, we propose a trajectory tracking control scheme for unmanned ships based on neural network observers, which has model uncertainty, unknown environmental disturbance and saturation problems. A neural network-based observer was developed to reconstruct unmeasured velocity and estimate the uncertainty of the model. Using the neural network, a neural adaptive output feedback controller was developed. In addition, a stable controller was designed by the backstepping method. Finally, the Lyapunov analysis shows that all signals in the closed-loop system are bounded. The feasibility of the proposed control scheme is verified by simulation.

1. Introduction

Autonomous surface vessels are utilized to reduce manual labor costs and enhance operational precision. Compared to manned marine vehicles, Autonomous surface vessels are more environmentally friendly toward marine ecosystems. Over the past decades, a significant number of Autonomous surface vessels have been employed in exploration, search, military, and surveillance operations. The widespread application of Autonomous surface vessels has been facilitated by rapid advancements in control theory and intelligent learning disciplines [1]-[2]. To successfully accomplish the tasks assigned to Autonomous surface vessels, researchers have conducted extensive studies in relevant technical fields, such as trajectory tracking, obstacle avoidance, and path planning, with trajectory tracking being one of the focal areas of research. Many challenges in this area still need to be addressed. At present, one of the main difficulties in the track tracking of unmanned surface vehicles lies in the fact that in the design process, in addition to obtaining the position of the unmanned vehicle, it is also necessary to have corresponding speed information. Although the position and heading information of Autonomous surface vessels can be readily obtained using Global Navigation Satellite Systems and gyroscopes, measuring speed might not be possible. Consequently, it is essential to explore the control issues of Autonomous surface vessels in the absence of speed measurements. Reference [3] introduced a passive nonlinear observer for Autonomous surface vessels, capable of reconstructing the vessel's speed and low-frequency motion. Reference [4] developed a hub motion estimation algorithm that utilizes sensor fusion from

Global Navigation Satellite Systems and Inertial Measurement Units. In reference [5], observer backstepping techniques were employed to design maneuvers for multiple unmanned vessels. However, these methods are based on the known parameters of the system model.

However, due to the complex and changeable working environment, it may be affected by factors such as wind, waves, and currents. Therefore, it is essential to consider the uncertainties of unmanned vessels in controller design. Neural networks (NN) have outstanding approximation and learning capabilities and have become a powerful and popular tool for estimating model uncertainties in nonlinear systems, as referenced in [6]. In reference [7], an adaptive neural network controller is proposed, employing a high-gain observer to estimate the uncertainties of unmanned vessels. In reference [8], a neural adaptive output feedback tracking controller was developed using a linear observer to update the neural network parameters. In reference [9], neural network prediction was utilized to estimate environmental disturbances affecting unmanned vessels.

In practical engineering applications, saturation is a common nonlinear characteristic of drives. At the same time, saturation nonlinearity is unavoidable in most drives, mainly including saturation limits of input amplitude and rate. In order to solve this kind of problem, in reference [10]-[12], a general driver compensation algorithm is proposed to control the input saturation problem. In reference [13], an observer-based anti-saturation compensator is proposed. In reference [14], Liu et al. studied the design of an adaptive controller for a single-input-single-output nonlinear system with parameter uncertainty and forced the system to be constrained, and constructed two parametric adaptive controllers using Nussbaum gain technology to overcome the unknown control direction problem. In reference [15], Chen et al. proposed a dynamic surface control method for a class of uncertain strict feedback nonlinear systems with input saturation and unknown external disturbances, and simulated the effectiveness of the dynamic surface control scheme under input saturation control.

In this paper, the unmanned ship tracking problem with model uncertainty, time-varying environmental interference and input saturation is studied. It proposes a neural adaptive output feedback control scheme. The unmanned vessels are interconnected via a directional communication network. The neural network observer not only identifies unknown model dynamics but also reconstructs unmeasured velocity information. On this basis, the method of combining tracking error transformation and boundary function is used to deal with the input saturation of the system. A kinematic control method based on velocity estimation and inertial constraint function was designed. Additionally, based on the estimated velocity and backstepping method, a kinematic control law is proposed. Finally, the neural network is used to establish the dynamic control law of the unmanned ship. Stability analysis using Lyapunov functions indicates that all error signals in the closed-loop system are bounded. The simulation results demonstrate the feasibility of the proposed method.

The organization of this paper is as follows. Section 1 introduces the research status of trajectory tracking of unmanned ships. Section 2 establishes the unmanned vessel model and related formulas, while Section 3 provides some necessary preliminary preparations and problem statements. Section 4 proposes a design scheme for the output feedback controller and presents a stability analysis. Section 5 provides a simulation to illustrate the theoretical results. Section 6 summarizes the paper.

2. Mathematical Model

2.1. Notatiaon

The following symbols will be used throughout this paper, $|\circ|$ representing absolute values unless specified otherwise. $\lambda_{\min}$ denotes the smallest eigenvalue of a matrix, and $\lambda_{\max}$ the largest eigenvalue of a matrix, respectively. $\|\circ\|$ represents the Euclidean norm. $\|\circ\|$ indicates the Frobenius norm, $R^{m\times n}$ representing $m\times n$ Euclidean space. $diag\{a_j\}$ signifies a block diagonal matrix, where a_j is the jth diagonal element. $(\circ)^T$ and $(\circ)^{-1}$ respectively denote the transpose and the inverse of a matrix. $\otimes$ represents the Kronecker product of matrices. $tr(\circ)$ indicates the trace of the corresponding matrices.

2.2. Neural Network Model

In this paper, a neural network approximation method based on radial basis functions is proposed, which can be used to estimate the model uncertainty and external interference by model the excitation functions of the nonlinear basis functions of the input layer, the hidden layer and the output layer. Given a positive number $\bar{\varepsilon}$ and a continuous function $f(\varsigma)$, $R^n \to R^k$ it can be approximated by a neural network radial basis function:

$$f(\varsigma) = W^T h_j(\varsigma) + \varepsilon(\varsigma), \forall \varsigma \in \Omega\varsigma, j = 1, 2, \ldots m \tag{1}$$

Where $\varepsilon(\varsigma) \in R^k$ represents the estimation error, satisfying $\|\varepsilon(\varsigma)\| \le \bar{\varepsilon}$. ς is the input vector, m is the number of neurons in the hidden layer, and $W \in R^{m\times k}$ are the interconnection weights from the hidden layer to the output, bounded by $\|W\|_F \le W^*$ where W^* is a positive constant. $h_j(\varsigma) \in R^m$ represents the vector of bounded neuron basis functions, $\|h_j\| \le \bar{h}$, where each $\bar{h}$ is a positive constant. Typically, $h_j(\varsigma)$ is selected as a Gaussian function, expressed as:

$$h(\varsigma) = \exp\left[\frac{\|\varsigma - c_j\|^2}{b_j^2}\right] \tag{2}$$

Where $c_j \in R^n$ and $b_j > 0$ is the center and width of the jth kernel unit, respectively.

Generally, the optimal weight vector W is unknown and needs to be estimated during the controller design. Let $\hat{W}$ be the estimate of W and define the weight estimation error as $\tilde{W} = \hat{W} - W$. Select the optimal weight vector W such that $\varepsilon(\varsigma)$ is minimized, defined as: $W = \arg\min_{\hat{W}\in R^{n\times m}} \{\sup_{\varsigma\in\Omega_\varsigma} | f(\varsigma) - \hat{W}^T h_j(\varsigma)|\}$.

2.3. Unmanned Vessel Model

This ship motion is described by six degrees of freedom, namely surge, sway, yaw, heave, roll, and pitch. To simplify the complexity of ship motion control, only the motion in the horizontal plane, comprising the three degrees of freedom-surge, yaw, and sway-is typically considered. To quantitatively describe the motion of these three degrees of freedom, two coordinate systems are commonly used: one is the body-fixed frame, which takes the ship itself as the reference point; the other is the earth-fixed frame, which uses the earth as the reference point. As illustrated in Figure 1.

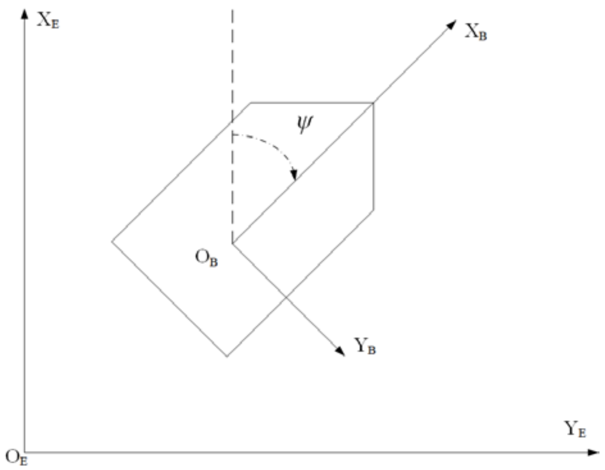

Figure 1: Body-fixed frame BO_BY_B and earth-fixed frame $X_EO_EY_E$

The mathematical model describing the motion of the unmanned vessel on the horizontal plane is expressed as follows[16]:

$$\begin{aligned}\dot{\eta} &= R(\psi)v \\ M\dot{v} &= -C(v)v - D(v)v + d + \tau + \tau_w\end{aligned} \tag{3}$$

Where $\eta=[x,y,\psi]^T$ represents the vector of vessel position (x,y) and heading angle ψ, and $v=[u,v,r]^T$ denotes the vector of surge, sway, and yaw velocities in the body-fixed frame. $\tau_w=[\tau_{w1},\tau_{w2},\tau_{w3}]^T$ represents the vector of environmental disturbances, and $R(\psi)$ is the rotation matrix, which satisfies $\|R(\psi)\|=1$, $R^T(\psi)R(\psi)=I_{3\times3}$, with its time derivative given by $R(\psi)=rR(\psi)S$, where $R(\psi)$ is the angular velocity matrix expressed as:

$$R(\psi)=\begin{bmatrix}\cos(\psi) & -\sin(\psi) & 0\\ \sin(\psi) & \cos(\psi) & 0\\ 0 & 0 & 1\end{bmatrix}$$

$$S=\begin{bmatrix}0 & -1 & 0\\ 1 & 0 & 0\\ 0 & 0 & 0\end{bmatrix} \tag{4}$$

For brevity in the following description, we omit ψ, $R=R(\psi)$, $\dot{R}=\dot{R}(\psi)$, $R^T=R^T(\psi)$. $\tau=[\tau_u,\tau_v,\tau_r]^T$ is the control vector of the vessel, comprising surge force τ_u, sway force τ_v, and yaw moment τ_r.

$$\tau=\begin{cases}\tau_{\max}, & \text{if } \tau_c>\tau_{\max}\\ \tau_c, & \text{if } \tau_{\min}\le\tau_c\le\tau_{\max}\\ \tau_{\min}, & \text{if } \tau_c<\tau_{\min}\end{cases} \tag{5}$$

Where, $\tau_{\max}\in R^3$, $\tau_{\min}\in R^3$ denote the maximum and minimum control forces and torques generated by the thrusters. $\tau_c=[\tau_{c1},\tau_{c2},\tau_{c3}]^T$ The controller computes accordingly.

The control objective of this paper is to design an output feedback controller for surface unmanned vessels that provides tracking of reference signals η_d despite model uncertainties and output constraints, using only position measurements η. Specifically, the goals are as follows:

1) To maintain the unmanned vessel in the required formation and track the reference signal η_d.

$$\lim_{t\to\infty}\|\eta-\eta_d\|\le o \tag{6}$$

Where o is a positive constant that can be made sufficiently small by selecting appropriate control parameters.

Prior to the design, we make the following assumptions:

Assumption 2 [17]: The time-varying environmental disturbances τ_w are bounded, $|\tau_w|\le\overline{\tau}_w$ where $\overline{\tau}_w$ is a positive constant.

Assumption 3: The reference signals η_d and $\dot{\eta}_d$ are bounded.

3. Extended State Observer Design

In actual navigation, parameters M, D, and C are difficult to determine, and the environmental disturbance and model uncertainty are unknown and unmeasurable, and the unknown environmental disturbance and model uncertainty information are estimated by introducing a state observer. The system models (3) is rewritten as

$$\dot{\eta}=Rv \tag{7}$$

$$M\dot{v}=\tau-f(v) \tag{8}$$

Where $\overline{M}^T=\overline{M}$ is the positive definite nominal inertia matrix, and $f(v)=(I_{3\times3}-\overline{M}M^{-1})\tau+\overline{M}M^{-1}(D(v)+C(v)v-\tau_w)$ encapsulates the model uncertainties and unknown environmental disturbances. Definition $f(v)=[f_1,f_2,f_3]^T$: As velocity v is unavailable, $f(v)$ it cannot be directly reconstructed using RBFNN. Here, the inputs τ and outputs η are used to reconstruct the unknown functions, where:

$$f(v)=W^T h_j(\varsigma)+\varepsilon(\varsigma) \tag{9}$$

Where $W\in R^{m\times3}$, $j=1,\ldots,$ and m represents the jth hidden layer neuron, with $\varsigma=[\eta^T,\eta^T(t-t_d),\eta^T(t-2t_d),\tau^T]^T$, $t_d>0$, $h_j(\varsigma)\in R^{m\times1}$, $\|\varepsilon(\varsigma)\|\le\overline{\varepsilon}$, and $\overline{\varepsilon}$ being positive constants.

Let $\hat{\eta}=[\hat{x},\hat{y},\hat{\psi}]^T$ and $\hat{v}=[\hat{u},\hat{v},\hat{r}]^T$ denote the estimated values of position η and velocity v, respectively. Define the position estimation error as $\tilde{\eta}=\hat{\eta}-\eta$, and design the neural network state observer as:

$$\dot{\hat{\eta}}=R\hat{v}-K_{o1}\tilde{\eta} \tag{10}$$

$$\overline{M}\dot{\hat{v}}=-\tilde{W}^T h_j(\varsigma)-\varepsilon(\varsigma)-K_{o2}R^T\tilde{\eta} \tag{11}$$

Where K_{o1},K_{o2} is the observer gain matrix to be designed.

The update law for $\hat{W}$ is designed as:

$$\dot{\hat{W}}=\gamma h_j(\varsigma)\tilde{\eta}^T R-\rho\hat{W} \tag{12}$$

Where $\rho,\gamma\in R$ is a designated positive constant.

Define the velocity estimation error as $\tilde{v} = \hat{v} - v$. Thus, the observer error dynamics can be written as:

$$\dot{\hat{\eta}} = R\hat{v} - K_{o1}\tilde{\eta}s \tag{13}$$

$$\bar{M}\dot{\hat{v}} = -\tilde{W}^T h_j(\varsigma) - \varepsilon(\varsigma) - K_{o2}R^T\tilde{\eta} \tag{14}$$

Define the observer error state as a new vector $X = [\tilde{\eta}^T, \tilde{v}^T]^T$ and rewrite the state observer error dynamics (13) and (14) as:

$$\dot{X} = AX + B(-\tilde{W}^T h_j(\varsigma) + \varepsilon(\varsigma)) \tag{15}$$

$$\tilde{\eta} = C_o X \tag{16}$$

Where

$$A = \begin{bmatrix} -K_{o1} & R \\ -K_{o2}\bar{M}^{-1}R^T & 0_{3\times3} \end{bmatrix}, B = \begin{bmatrix} 0_{3\times3} \\ \bar{M}^{-1} \end{bmatrix}$$
$$C_{o1} = \begin{bmatrix} I_{3\times3} & 0_{3\times3} \end{bmatrix} \tag{17}$$

A depends on nonlinear terms R making the stability analysis of the designed observer challenging. Thus, a transformation $\chi = TX$ and $T = diag\{R^T, I_{3\times3}\}$, such that:

$$\dot{\chi} = (A_0 + rS_T)\chi + B(-\tilde{W}^T h_j(\varsigma) + \varepsilon(\varsigma)) \tag{18}$$

Where $S_T = diag\{S^T, 0_{3\times3}\}$.

$$A_0 = \begin{bmatrix} -K_{o1} & I_{3\times3} \\ -K_{o2}\bar{M}^{-1} & 0_{3\times3} \end{bmatrix} \tag{19}$$

Lemma 2: If parameters satisfy $(\rho / 2\gamma) - (\bar{h}_j^2 / 2) > 0$ and there exists a symmetric positive definite matrix $Q, P \in R^{6\times6}$, then the observer estimation error signal is bounded, satisfying the inequality:

$$A_0^T P + PA_0 + PBB^T P + Q + FF^T + \bar{r}(S_T^T P + PS_T) \le 0 \tag{20}$$

$$A_0^T P + PA_0 + PBB^T P + Q + FF^T - \bar{r}(S_T^T P + PS_T) \le 0 \tag{21}$$

Where $\bar{r} \in R$ is the upper bound of r. $F = C_0^T - PB$
Considering the Lyapunov equation:

$$V_0 = \frac{1}{2}\chi^T P\chi + \frac{1}{2\gamma}tr(\tilde{W}^T\tilde{W}) \tag{22}$$

Substituting equations (12), (18) into the above results in:

$$
\begin{aligned}
\dot{V}_0 &= \chi^T P \dot{\chi} + \frac{1}{\gamma} tr(\tilde{W}^T \dot{\tilde{W}}) \\
&= \chi^T P((A_0 + rS_T)\chi + B(-\tilde{W}^T h_j(\varsigma) + \varepsilon(\varsigma))) + \frac{1}{\gamma} tr(\tilde{W}^T \dot{\tilde{W}}) \\
&\le \chi^T P((A_0 + rS_T)\chi + B(-\tilde{W}^T h_j(\varsigma) + \varepsilon(\varsigma))) + \frac{1}{\gamma} tr(\tilde{W}^T \dot{\hat{W}}) \\
&\le \chi^T P(A_0 + rS_T)\chi - \chi^T F \tilde{W}^T h_j(\varsigma) + \chi^T PB\varepsilon(\varsigma) - \frac{\rho}{\gamma} tr(\tilde{W}^T \dot{\hat{W}})
\end{aligned} \tag{23}
$$

Where $-tr(\tilde{W}^T \dot{\hat{W}}) \le -\frac{1}{2} \| \tilde{W} \|_F^2 + \frac{1}{2} \| W \|_F^2$, $\chi^T PB\varepsilon(\varsigma) \le \frac{1}{2} \chi^T PBB^T P \chi + \frac{1}{2} \varepsilon^2(\varsigma)$, $-\chi^T F \tilde{W}^T h_j(\varsigma) \le \frac{1}{2} \chi^T FF^T \chi + \frac{1}{2} \tilde{W}^T h_j(\varsigma) h_j^T(\varsigma)$ combining equations (20), (21), (23), it can be derived:

$$
\begin{aligned}
\dot{V}_0 &\le -\lambda_{\min}(Q) \| \chi \|^2 - \left(\frac{\rho}{2\gamma} - \frac{\bar{h}_j^2}{2} \right) \| \tilde{W} \|_F^2 + \frac{\rho}{2\gamma} \| W \|_F^2 + \frac{1}{2} \varepsilon^2(\varsigma) \\
&\le -c_2 V_0 + c_1
\end{aligned} \tag{24}
$$

Where $c_1 = \rho / 2\gamma \| W \|_F^2 + 1/2 \| \bar{\varepsilon}(\varsigma) \|^2$, $c_2 = \min\{2\lambda_{\min}(Q)/\lambda_{\max}(P), \rho - \gamma \bar{h}_j^2\}$. Therefore, the state χ is bounded, $T^T = T^{-1}, \| T^T \| \le 1, X = T^T \chi$ and consequently, the estimation error signal is also bounded.

4. Controller Design

The controller design process includes two steps.
Step 1: Define the first error vector based on the communication topology.

$$
z_1 = \eta - \eta_d \tag{25}
$$

z_1 Deriving with respect to time yields:

$$
\dot{z}_1 = Rv - \dot{\eta}_d \tag{26}
$$

In (26), v is chosen as the virtual input, and the kinematic control law β can be written as:

$$
\beta = -R^{-1}(K_1 z_1 - \dot{\eta}_d) \tag{27}
$$

Where $K_1 \in R^3$ is the diagonal gain matrix to be designed.
Step 2: In this step, define the second error vector as:

$$
z_2 = v - \bar{\beta} - \theta\alpha \tag{28}
$$

Where $\theta \in R^3$ is a positive definite matrix, α is an auxiliary dynamic variable, and $\bar{\beta}$ is the signal from the β signal input to the first-order filter. $\bar{\beta}$ is given by the following formula

$$
l\dot{\bar{\beta}} + \bar{\beta} = \beta \tag{29}
$$

Where $l \in R^3$ is a positive definite matrix.

Combining equation (3), the time derivative of z_2 is derived as

$$\dot{z}_2 = \xi + M^{-1}(\tau_c - \varpi) - \dot{\bar{\beta}} - \theta\dot{\alpha} \tag{30}$$

The error function between unsaturated and saturated problems is defined as $\varpi = [\varpi_u, 0, \varpi_r]$.

Where $\xi = [\xi_1, \xi_2, \xi_3]^T \in R^3$ is used to represent total disturbances, it is a state vector expressed as

$$\xi = M^{-1}(-C(v)v - D(v)v + d) \tag{31}$$

The dynamic update rate of auxiliary variable α is designed as follows

$$\dot{\alpha} = -\theta^{-1}(T\alpha + M^{-1}\varpi) \tag{32}$$

Where T is the gain matrix of α.

To ensure stability z_2, the dynamic control law is designed as

$$\tau_c = M(-K_2 z_2 - R^T z_1 + \dot{\bar{\beta}} - T\alpha - \hat{\xi}) \tag{33}$$

Where K_2 is the gain matrix of τ_c.

The following theorem is presented to indicate the stability of the entire closed-loop system.

Theorem 1: The proposed neural adaptive output feedback control scheme guarantees that: 1) all signals in the closed-loop system are bounded. 2) The unmanned vessel is capable of tracking a reference signal with bounded tracking error. 3) The output position of the unmanned vessel satisfies output constraints.

Proof: Select a Lyapunov function candidate as follows:

$$V_1 = \frac{1}{2}z_1^T z_1 + \frac{1}{2}z_2^T z_2 + \frac{1}{2}\tilde{\beta}^T\tilde{\beta} + \frac{1}{2}\alpha^T\alpha + V_0 \tag{34}$$

Where $\tilde{\beta} = \bar{\beta} - \beta$.

According to equations (25), (29), (30), (24), the derivative of time is obtained

$$\begin{aligned}\dot{V}_1 &= z_1^T(Rv - \dot{\eta}_d) + z_2^T(\xi + M^{-1}\tau - \dot{\bar{\beta}} - \theta\dot{\alpha}) \\ &\quad -\tilde{\beta}^T l^{-1}\dot{\tilde{\beta}} + \alpha^T\theta^{-1}(-T\alpha + M^{-1}\varpi) - c_2 V_0 + c_1\end{aligned} \tag{35}$$

Equations (27), (32) into equations (35) obtain

$$\begin{aligned}\dot{V}_1 &= -z_1^T K_1 z_1 - z_2^T K_2 z_2 - \tilde{\beta}^T l^{-1}\tilde{\beta} - \alpha^T\bar{T}\alpha \\ &\quad + z_1^T R(\tilde{\beta} + \theta\alpha) + \alpha^T\bar{M}\varpi - c_2 V_0 + c_1\end{aligned} \tag{36}$$

Where $\bar{T} = {}^T\theta^{-1}T$, $\bar{M} = {}^T\theta^{-1}M^{-1}$.

Using Young's inequality, the inequality is given by:

$$\begin{aligned}z_1^T R(\tilde{\beta} + \theta\alpha) &= z_1^T R\tilde{\beta} + z_1^T\theta\alpha \\ &\le [\lambda_{\max}(\theta) + 1]/2 z_1^T z_1 + 1/2\tilde{\beta}^T\tilde{\beta} + 1/2\alpha^T\alpha\end{aligned} \tag{37}$$

$$\alpha^T\bar{M}\varpi \le \lambda_{\max}(\bar{M})/2(\alpha^T\alpha + \varpi^T\varpi) \tag{38}$$

Let $k_1 = \lambda_{\min}(K_1) - [\lambda_{\max}(\theta) + 1]/2$, $k_2 = \lambda_{\min}(K_2)$, $k_3 = \lambda_{\min}(t^{-1}) - 1/2$, $k_4 = \lambda_{\min}(\bar{T}) - \lambda_{\max}(\bar{M})/2 - 1/2$, $c_3 = \lambda_{\max}(\bar{M})/2\varpi^T\varpi + c_1$. The Equation (38) can be rewritten as

$$\dot{V}_1 \le -k_1 z_1^T z_1 - k_2 z_2^T z_2 - k_3 \tilde{\beta}^T \tilde{\beta} - k_4 \alpha^T \alpha - c_2 V_0 + c_1 \tag{39}$$

Further simplification is available

$$\dot{V}_1 \le -2\mu_1 V_1 + c_3 \tag{40}$$

Where, $\mu_1 = \min\{k_1, k_2, k_3, k_4, c_2/2\}$.
Ultimately, it can be derived that:

$$V_1 \le [V_1(0) - \frac{c_3}{2\mu_1}]e^{-2\mu_1 t} + \frac{c_3}{2\mu_1} \tag{41}$$

From the formulation of V_1, we can know $t \to \infty$, $V_1 \to c_1/2\mu_1$, the convergence range of the Lyapunov function can be set by adjusting the parameters in variable μ_1. It can be concluded that z_1, z_2, α, $\tilde{\beta}$ and $\tilde{\xi}$ are bounded. Therefore, all signals in the closed loop are bounded.

5. Simulation Results

This section presents simulation results conducted in Matlab, which validate the effectiveness and feasibility of the controller. The initial position of the unmanned vessel was set at $\eta = [0.1\text{m}, 1\text{m}, \pi/4\text{rad}]^T$, with the required deviation configured as $v = [0\text{m}, 1.2\text{m}, 0\text{rad}]^T$. Initial estimates for position and velocity were set at $\hat{\eta}(0) = \eta(0)$ and $\hat{v}(0) = [0\text{m/s}, 0\text{m/s}, 0\text{rad/s}]^T$, Constraints on control forces and torques were set to $\tau_{1,\max} = -\tau_{1,\min} = 2N$, $\tau_{2,\max} = -\tau_{2,\min} = 2N$, and $\tau_{3,\max} = -\tau_{3,\min} = 1.5N$. The constraints k_b were established at $k_b = [0.5\text{m}, 0.6\text{m}, 0.15\text{rad}]$.

The observer for the unmanned vessel was designed according to equations (3), with observer parameters set to $K_{o1} = 30 \times \text{diag}\{1,1,1\}$, $K_{o2} = 30 \times \text{diag}\{1,1,1\}$. The controller was designed as per equation (33), with parameters $K_1 = 2.2 \times \text{diag}\{1,1,1\}$, $K_2 = \text{diag}\{60,60,23\}$ configured. The update rate $\hat{W}$ was set according to equation (12), with parameters defined $\gamma = 1000$, $\rho = 0.2$.

The simulation results are illustrated in Figures 2 to 4. Figure 2 displays the reference trajectory alongside the tracking trajectory, where the blue solid line represents the reference trajectory and the red dashed line represents the tracking trajectory. It is observable that, after initial fluctuations, the unmanned vessel accurately tracks the set trajectory. Figure 3 presents the tracking error curve, despite initial deviations, the final tracking error converges to a small neighborhood around zero. Figure 4 depicts the velocity estimation curve. From Figure 4, we can see that the trajectory of the unmanned ship is shaking, and because when the input of the arctangent function is close to the singularity, the control signal is abnormal, and the trajectory of the unmanned ship will jitter. This is also the problem that we need to solve in the next research.

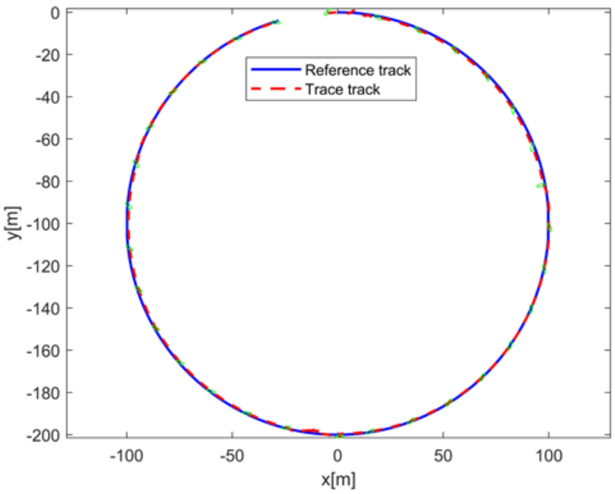

Figure 2: Reference track and trace track.

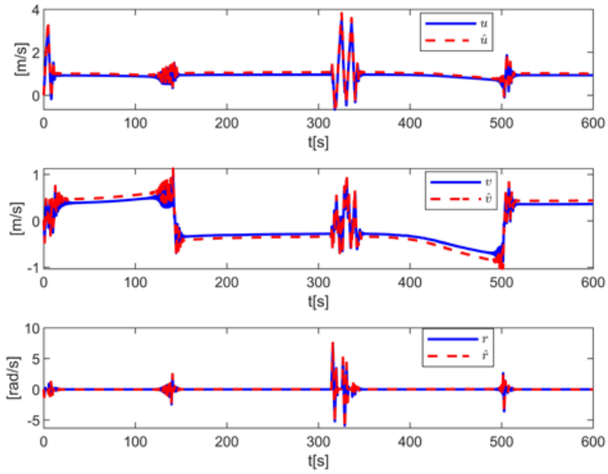

Figure 3: Velocity estimation curves.

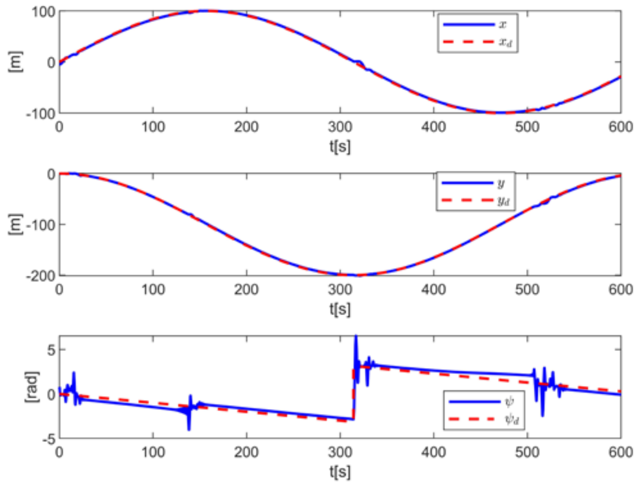

Figure 4: Position and heading tracking curves.

6. Conclusions

In this paper, we addressed the challenges of output feedback formation tracking control for unmanned vessels in the presence of model uncertainties, unknown environmental disturbances, and input constraints. A neural network state observer was proposed, enabling the simultaneous estimation of unmeasured velocities and unknown model dynamics. Additionally, based on the estimated velocity and backstepping method, a kinematic control law is proposed. Finally, the neural network is used to establish the dynamic control law of the unmanned ship. Stability analysis using Lyapunov functions indicates that all error signals in the closed-loop system are bounded. Simulation and comparative results validated the tracking performance of the proposed distributed controller.

References

[1] Caccia M, Bibuli M, Bono R et al. Basic navigation, guidance and control of an unmanned surface vehicle [J]. Autonomous Robots, 2008, 25(4): 349-365.

[2] Fossen T I. Handbook of marine craft hydrodynamics and motion control [M]. West Sussex: Wiley, 2011.

[3] I. F. Ihle, R. Skjetne, and T. I. Fossen, Output feedback control for maneuvering systems using observer backstepping, in Proc. IEEE Int. Symp, Mediterrean Conf. Control Automat. Intell. Control, Jun. 2005, pp. 15121517.

[4] S. S. Ge, C. C. Hang, and T. Zhang, Adaptive neural network control of nonlinear systems by state and output feedback, IEEE Trans. Syst, Man, Cybern B, Cybern, vol. 29, no. 6, pp. 818828, Dec. 1999.

[5] G. Xia, H. Wu, and X. Shao, Adaptive filtering backstepping for ships steering control without velocity measurements and with input con straints, Math. Problems Eng., vol. 2014, Mar. 2014, Art. no. 218585.

[6] G. Wen, S. S. Ge, C. L. P. Chen, F. Tu, and S. Wang, Adaptive tracking control of surface vessel using optimized backstepping technique, IEEE Trans. Cybern, vol. 49, no. 9, pp. 34203431, Sep. 2019.

[7] J. Du, X. Hu, H. Liu, and C. L. P. Chen, Adaptive robust output feed back control for a marine dynamic positioning system based on a high gain observer, IEEE Trans. Neural Netw Learn Syst, vol. 26, no. 11, pp. 27752786, Nov. 2015.

[8] L.-J. Zhang, H.-M. Jia, and X. Qi, NNFFC-adaptive output feedback trajectory tracking control for a surface ship at high speed, Ocean Eng., vol. 38, no. 13, pp. 1430 1438, 2011.

[9] Z. Peng, D. Wang, H. H. Liu, G. Sun, and H. Wang, Distributed robust state and output feedback controller designs for rendezvous of networked autonomous surface vehicles using neural networks, Neurocomputing, vol. 115, pp. 130141, Sep. 2013.

[10] Boscolo I, Colson WB, Small Gain Formula and Saturation in an Optical klystron Freen physics Electron Laser. Nuclear instruments and methods research, 1984: 237(1-2):118-123.

[11] Guan W, Yang G H, Analysis and design of output feedback control systems with actuator saturation, Journal of Control Theory and Applicatons, 2008.6(4):421-426.

[12] Teel A R. Nonlinear small gain theorem of the analysis of control systems with saturation. IEEE Transactions on Automatic Control, 1996:4 (9): 1256-1270.

[13] Walgama K S and Sternby J. inherent observer property in a class of anti-windup compensator. Int. J. Control, 1990, 52(3):705-724.

[14] Liu Y J, Tong S. Barrier Lyapunov functions for Nussbaum gain adaptive control of full state constrained nonlinear systems[J]. Automatic, 2017, 76: 143-152.

[15] Chen M, Tao G, Jiang B. Dynamic surface control using neural networks for a class of uncertain nonlinear systems with input saturation[J]. IEEE transactions on neural networks and learning systems, 2014, 26(9): 2086-2097.

[16] T. I. Fossen, Marine Control Systems Guidance, Navigation, and Control of Ships, Rigs and Underwater Vehicles, 1st ed. Trondheim, Norway: Marine Cybernetics, 2002.

[17] G. Xia, C. Sun, B. Zhao, and J. Xue, Cooperative control of multiple dynamic positioning vessels with input saturation based on finite time disturbance observer, Int. J. Control, Autom. Syst., vol. 17, no. 2, pp. 370379, Feb. 2019.